Supporting Information

Ultra-trace electrochemical determination of total arsenic in actual water samples and food matrices using nano-granular gold-copper modified glassy carbon electrode (NG-AuCu/GCE)

Sadia Yousaf [a], Usman Naseer[b], Mehwish Shah[a], Liufang Chen[a], Hailong Yan[a, *], Qingyun Cai[a, *]

[a]State Key Laboratory of Chemo and Biosensing, College of Chemistry and Chemical Engineering, Hunan University, Changsha 410082, P. R. China

[b]Department of Public Health, Monroe University, King Graduate School, NY 10468, United States.

Correspondence; Hailong Yan, Qingyun Cai, State Key Laboratory of Chemo and Biosensing, College of Chemistry and Chemical Engineering, Hunan University, Changsha 410082, P. R. China

Email: yanhailong@hnu.edu.cn; qycai0001@hnu.edu.cn

1. Optimization of electrochemical deposition

Initially, optimization of parameters in the precursor solution was performed, namely the Au–Cu ratio and the electrochemical deposition time on the GCE surface, to achieve the best performance of NG-AuCu/GCE for total arsenic determination and stability, even in acidic environments. For this purpose, Au–Cu ratio and electrochemical deposition time (electroplating time) were optimized.

First, electrodeposition time was optimized and the obtained sensor was used to detect 100 ppb arsenic to evaluate the optimal performance. Electrodeposition time serves as a crucial parameter, which is intimately related to the active surface area of the modified NG-AuCu/GCE. During the electrodeposition of AuCu nanogranules, a series of electrodeposition times were investigated. The peak current for As(III) increased from 300 s to 1200 s and then declined at 1800 s, with maximum efficiency achieved at 1200 s. Therefore, 1200 s was chosen as the optimal electrodeposition time (Fig. S1).

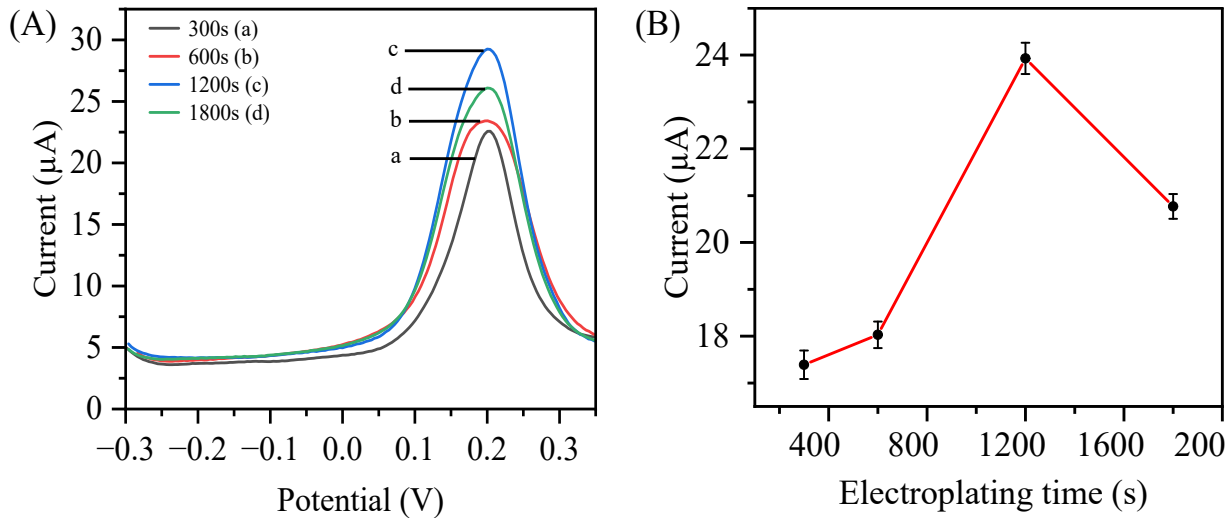

Fig. S1. Optimization of electrochemical deposition time for the NG-AuCu/GCE. (A) SWASV responses for 100 ppb As(III) at different electrodeposition times, and (B) Plot of arsenic peak current vs. electrodeposition time.

It was observed that when the electrodeposition time was gradually increased from 300 to 1200 s, the concentration of gold ions gradually decreased, leading to a reduction in the size of crystal grains in the solution [1] and resulting in the deposition of a well-defined nanogranular network on the GCE surface. When the electrodeposition time was further increased, the structure

became more compact, and the coating layer of the nanoparticles became thicker. Therefore, excessive electrodeposition time (1800 s) led to the stripping of nanoparticles from the surface of the GCE, thereby decreasing the active surface area of the GCE for As(III) detection [2].

The second most crucial factor to optimize is the gold–copper ratio (Au–Cu ratio) in the precursor solution used for electrodeposition. Five distinct ratios (5:1, 2:1, 1:1, 1:2, and 1:5) were tested (Fig. S2).

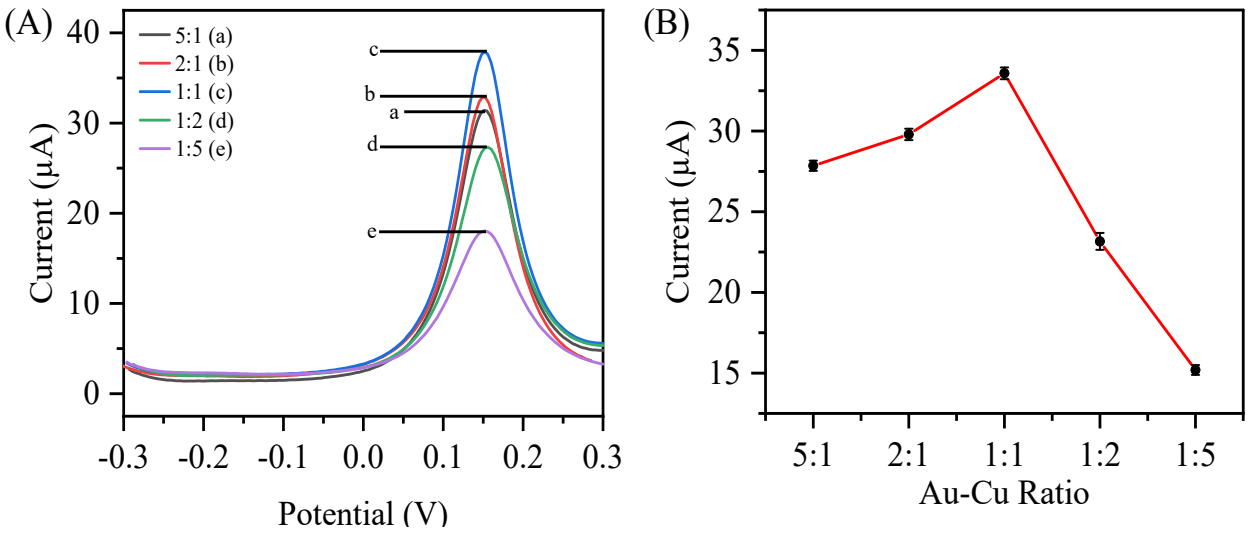

Fig. S2. Optimization of Au-Cu ratio in electrochemical deposition solution to synthesize the NG-AuCu/GCE. (A) SWASV responses for 100 ppb As(III) obtained from the sensor fabricated with different Au-Cu ratio, and (B) Corresponding plot of arsenic peak current vs. Au-Cu ratio.

It was observed that when the Au–Cu ratio was 5:1 or 2:1, the peak current was favorable but lower than that at 1:1. As the ratio shifted from 1:1 to 1:2 and 1:5, the peak current for arsenic decreased. It is clearly demonstrated that 1:1 was the optimal choice. Consequently, this ratio was selected for all subsequent measurements. With an increase in gold concentration, there was a loss of synergistic enhancement, resulting in a lower response for arsenic. Additionally, increasing the concentration of gold resulted in a smoother surface and a reduced surface area by blocking the active sites of copper for catalytic reactions. It has been reported that the size of AuCu nanogranules decreased with increasing copper content; however, an excess of copper ions interferes with the electrochemical determination of arsenic by forming intermetallic compounds such as Cu_3As_2, leading to a decrease in the stripping current [3, 4].

2. Optimization of all voltammetric parameters (SWASV parameters)

The next step involves the optimization of the electrolyte used for As(III) determination. Initially, the three acids were tested at different concentrations (0.1 M, 0.5 M, 1 M, and 2 M), and H_2SO_4 performed best compared to HCl and HNO_3 (Fig. S3). The best-performing molar concentration of each acid was then selected for presentation in the final electrolyte optimization figure (Fig. S4). For optimization, NG-AuCu/GCE was tested in three electrolytes: 0.5 M H_2SO_4, 1 M HCl, and 1 M HNO_3. Based on the results, it was found that the peak current for arsenic in 0.5 M H_2SO_4 was higher than that in 1 M HCl and 1 M HNO_3, as it offers excellent conductivity and higher sensitivity for the modified sensor. Therefore, 0.5 M H_2SO_4 was chosen as the optimized supporting electrolyte for further measurements (Fig. S3 and Fig. S4).

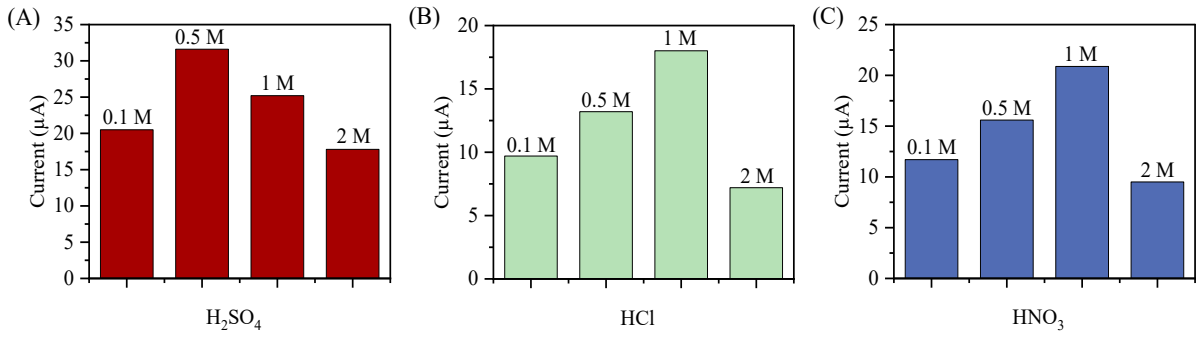

Fig. S3. SWASV responses of different electrolytes for 100 ppb As(III) using NG-AuCu/GCE at different molar concentrations. (A) H_2SO_4, (B) HCl, and (C) HNO_3.

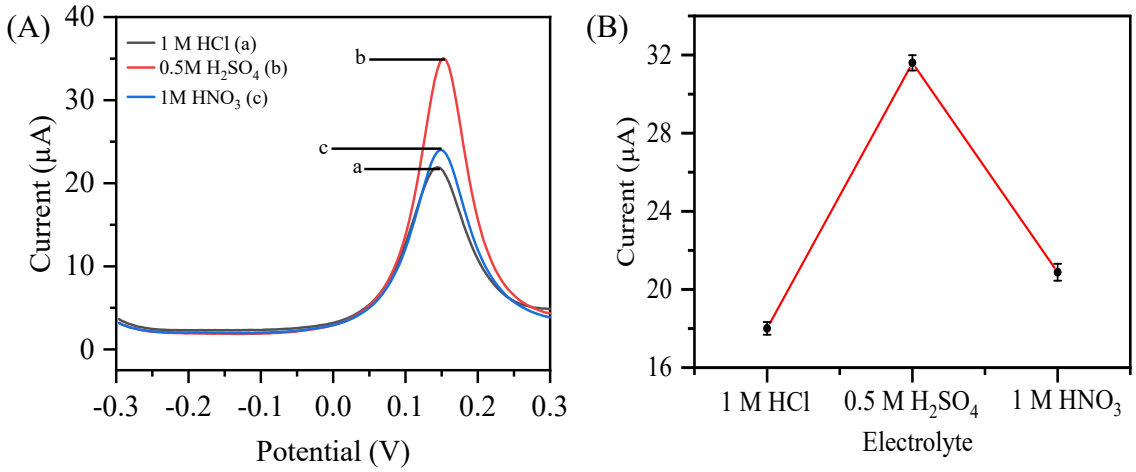

Fig. S4. Optimization of electrolyte solution for As(III) determination using NG-AuCu/GCE. (A) SWASV responses for 100 ppb As(III) obtained from the developed sensor for three different electrolyte solutions, and (B) Corresponding plot of arsenic peak current vs. electrolyte.

Additionally, the deposition potential was optimized through a series of experiments conducted at varying potentials ranging from -0.1 V to -0.5 V. The As(III) peak current initially increased and then decreased, with maximum efficiency observed at -0.3 V. The decrease in the oxidation peak current at potentials more negative than -0.3 V is attributed to hydrogen evolution [5]. Therefore, -0.3 V was selected as the optimal deposition potential for further studies in this work (Fig. S5).

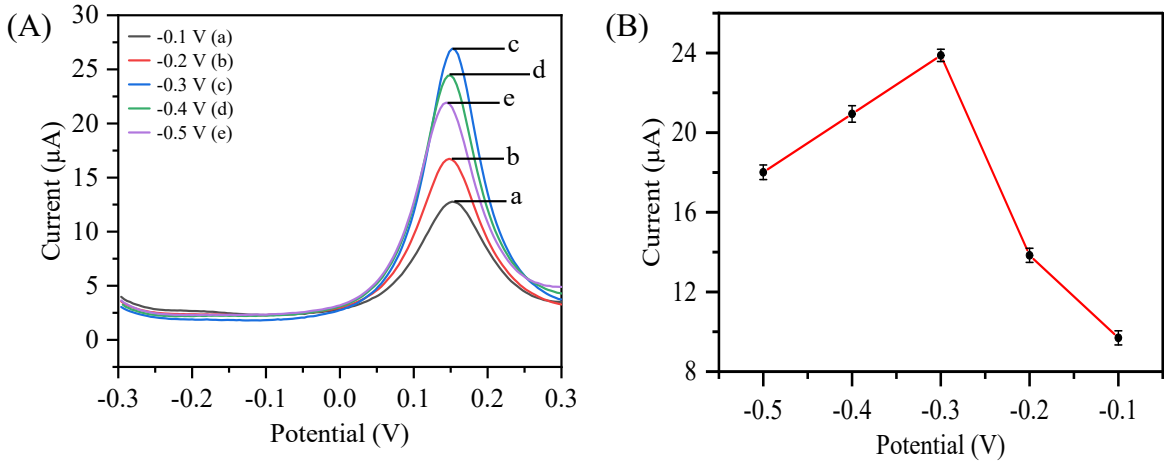

Fig. S5. Optimization of deposition potential for As(III) determination using NG-AuCu/GCE. (A) SWASV responses for 100 ppb As(III) obtained from the developed sensor at various deposition potential, and (B) Corresponding plot of arsenic peak current vs. deposition potential.

Next, the deposition time for As(III) determination by using SWASV was tested. Different deposition times (30 s, 60 s, 100 s, 120 s, and 200 s) were applied to detect 100 ppb As(III) in 0.5 M H_2SO_4 solution. The peak current was recorded and compared to obtain the best optimized deposition time (Fig S6).

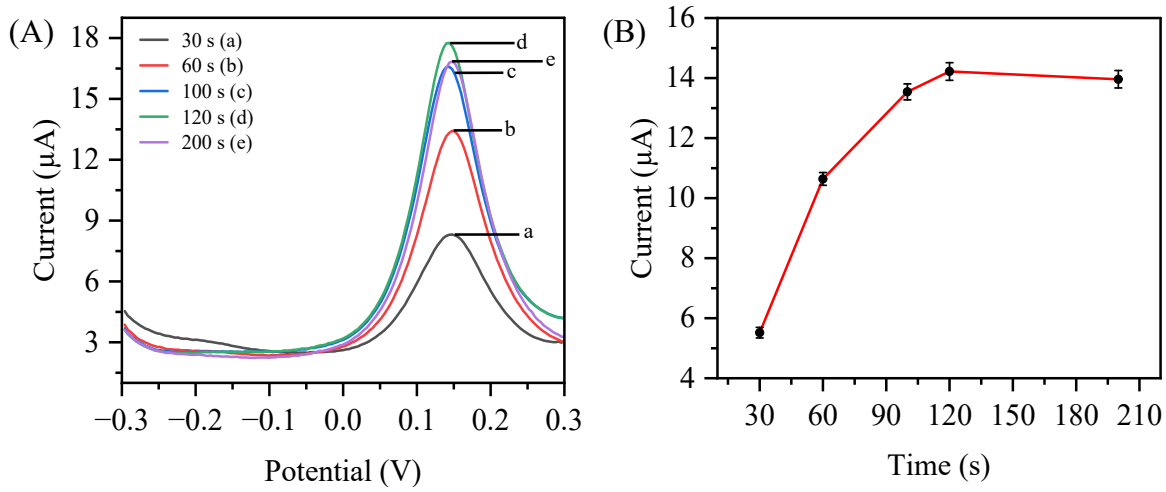

Fig. S6. Optimization of deposition time for As(III) determination using NG-AuCu/GCE. (A) SWASV responses for 100 ppb As(III) obtained from the developed sensor at various deposition time, and (B) Corresponding plot of arsenic peak current vs. deposition time.

The deposition time (accumulation time) for the determination of As(III) using SWASV was an important parameter to be optimized [6]. It was clearly indicated that the peak current for the determination of As(III) gradually increased as the deposition time was extended from 30 seconds to 200 seconds. However, after 120 seconds, the peak current slightly decreased. Therefore, an accumulation time of 120 seconds was selected as optimal for all subsequent measurements.

3. Structure and composition of NG-AuCu/GCE

Structure and composition of NG-AuCu/GCE were examined by SEM and EDS spectra before and after detecting arsenic in 0.5 M H_2SO_4 solution. It was observed that there was no obvious difference in surface morphology, and elemental mapping confirmed that the AuCu nanogranules remained on the surface of the modified sensor after arsenic detection, similar to their state before detection. This confirms that the modified sensor is stable and highly efficient for long-term use (Fig. S7).

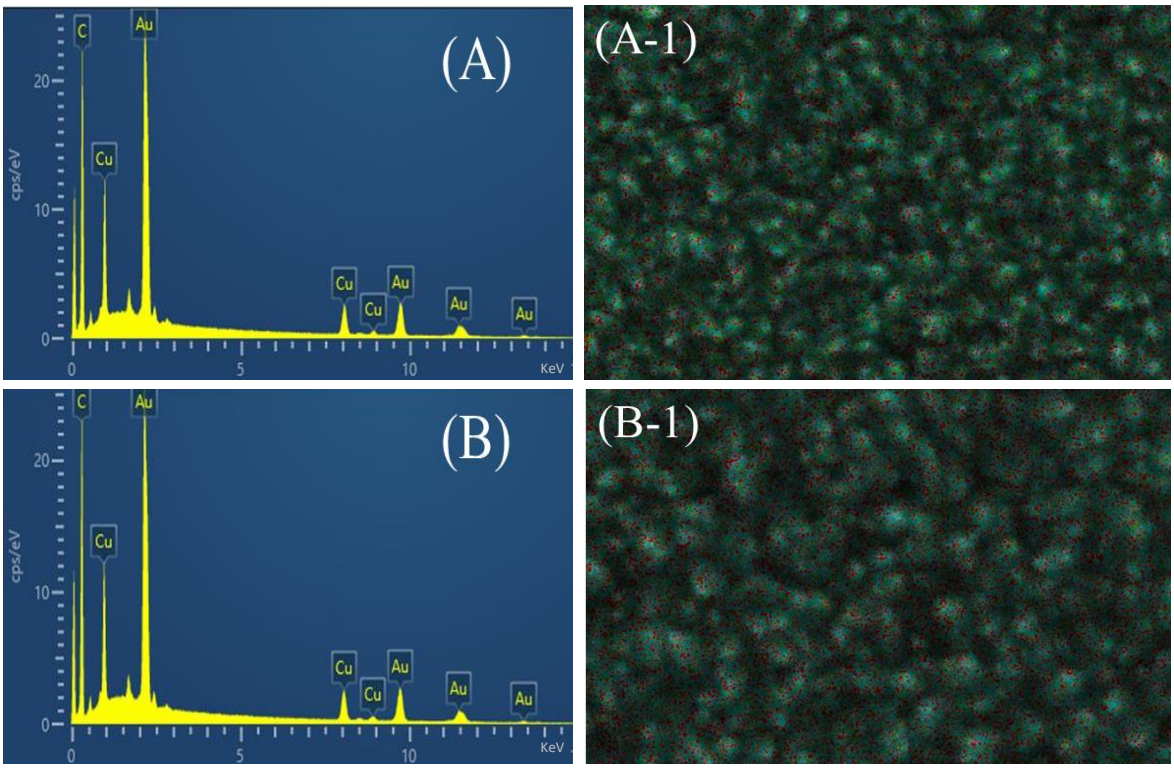

Fig. S7. (A and A-1) EDS spectra and elemental mapping analysis of AuCu/GCE before determining arsenic, (B and B-1) After determining arsenic in 0.5 M H_2SO_4 solution.

Furthermore, the electrochemically active surface area (ECSA) of NG-AuCu/GCE was calculated by Randles-Sevcik equation: $i_p = (2.69 \times 10^5) n^{3/2} A C D^{1/2} v^{1/2}$ [3, 7], where i_p is the peak current, n is the number of electrons (n = 1), A is the ECSA (cm^2), D is the diffusion coefficient ($cm^2\ s^{-1}$), C is the concentration of $[Fe(CN)_6]^{3-/4-}$ ($mol\ cm^{-3}$), and v is the scan rate (Vs^{-1}). Diffusion coefficient D was 6.7×10^{-6} $cm^2\ s^{-1}$ for the current study. The ECSA of bare GCE, NG-AuCu/GCE at the first day, and after 10-days stability test were 0.069 cm^2, 0.107 cm^2 and 0.105 cm^2, respectively (Fig. S8 and Fig. S9). The loss of ECSA was only 1.87%, indicating excellent stability of NG-AuCu/GCE (retaining almost all of its ECSA) over the period of ten days. From the above-mentioned results, it can be seen that NG-AuCu/GCE as a highly conductive sensor with a negligible loss of ECSA, confirming that the sensor's performance is maintained over the tested period. Therefore, NG-AuCu/GCE is suitable for long-term sensing with excellent stability.

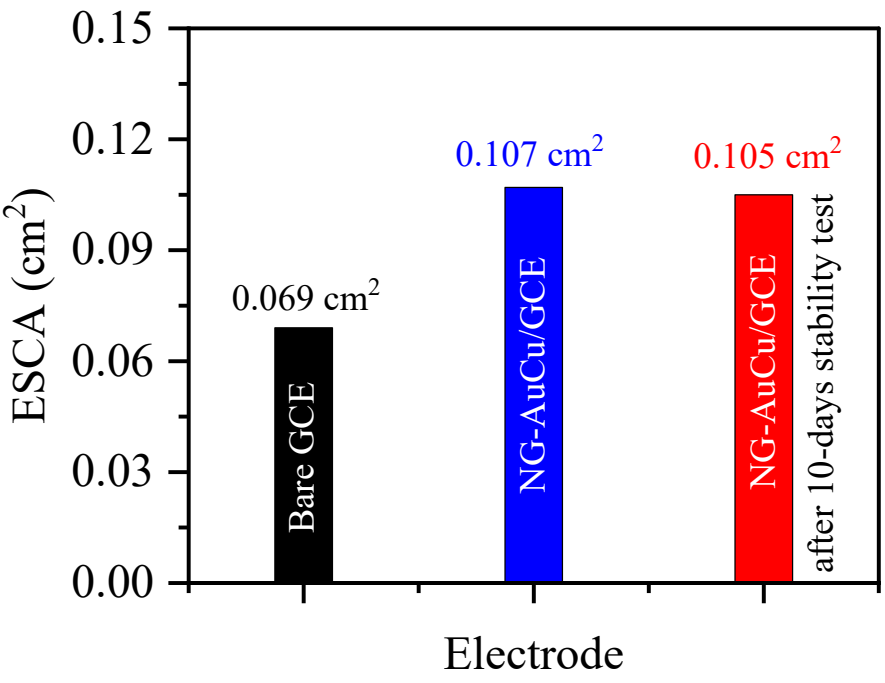

Fig. S8. A clear representation of ESCA comparison for bare GCE (black color), NG-AuCu/GCE at first day (blue color), and NG-AuCu/GCE after 10-days stability test performed (red color).

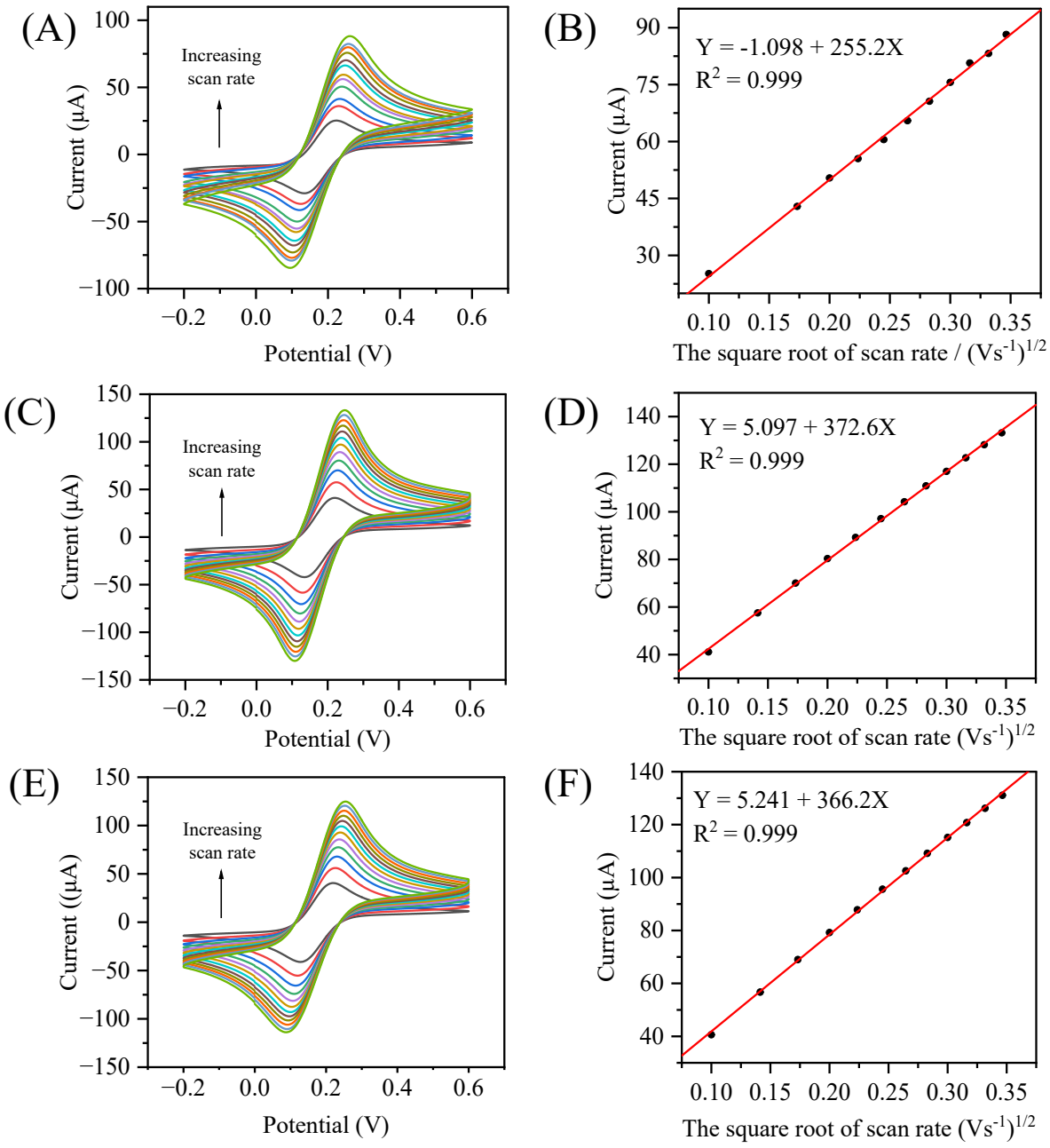

Fig. S9. Scan rate study (from 0.01 to 0.12 V s^{-1}) on NG-AuCu GCE, (A) bare GCE, (C) at the day one, and (F) after 10-days stability test in 5 mM $[Fe(CN)_6]^{3-/4-}$ solution containing 0.1 M KCl. (B, D, and F) the corresponding plot of current versus the square root of scan rate with a trendline.

4. Electrochemical measurements of arsenic determination

Another experiment was performed using NG-AuCu/GCE with As(III) concentrations ranging from 10 ppb to 100 ppb. All parameters were used under optimized conditions. The results are illustrated along with a calibration plot (Fig. S10).

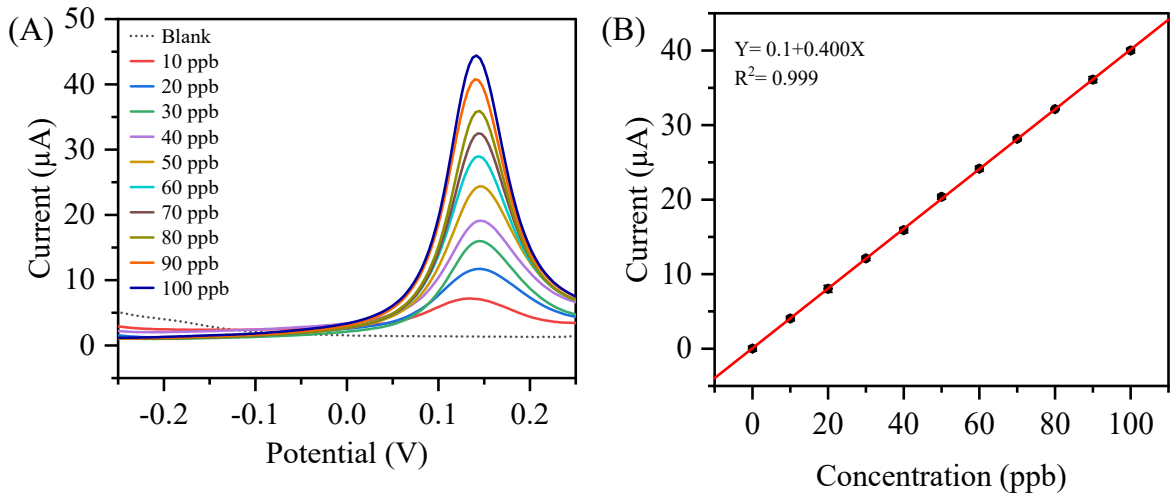

Fig. S10. SWASV responses of NG-AuCu/GCE for different concentrations of As(III) from 10 ppb to 100 ppb. (A) SWASV response of the NG-AuCu/GCE for As(III) determination (dotted line showing 0 ppb), and (B) Corresponding calibration plot of peak current for As(III) concentrations.

5. Real sample analysis

5.1 Tap water and mineral water

After sample preparation, 20 mL of the prepared sample (tap water and mineral water separately) was transferred into the electrochemical cell and deaerated by N_2 purging for 10 minutes prior to each measurement. The logarithm of the spiked arsenic concentration had a good linear relationship with logarithm of peak current under optimized conditions. The linear relationships between peak current and spiked arsenic for tap water and mineral water samples were $Y = 0.045 + 0.398X$ ($R^2 = 0.999$) and $Y = 0.031 + 0.408X$ ($R^2 = 0.999$) respectively (Fig. S11). Subsequently, specific As(III) concentrations (1, 5, and 30 ppb) were added to tap and mineral water samples. Arsenic was then determined based on the corresponding standard calibration equations obtained.

5.2 Fruit juice and apple peel

After sample preparation, 20 mL volume of prepared sample (fruit juice and apple peel separately) was poured into electrochemical cell and deaerated by N_2 purging for 10 minutes prior to each measurement. The logarithm of the spiked arsenic concentration had a good linear relationship with logarithm of peak current under optimized conditions. The linear relationships between peak current and spiked arsenic for fruit juice and apple peel samples were $Y = 0.0139 + 0.426X$ ($R^2 = 0.997$) and $Y = 0.392 + 0.383X$ ($R^2 = 0.996$), respectively (Fig. S12). Subsequently,

specific As(III) concentrations (10, 20, and 50 ppb) were added to tap and mineral water samples. Arsenic was then determined based on the corresponding standard calibration equations obtained.

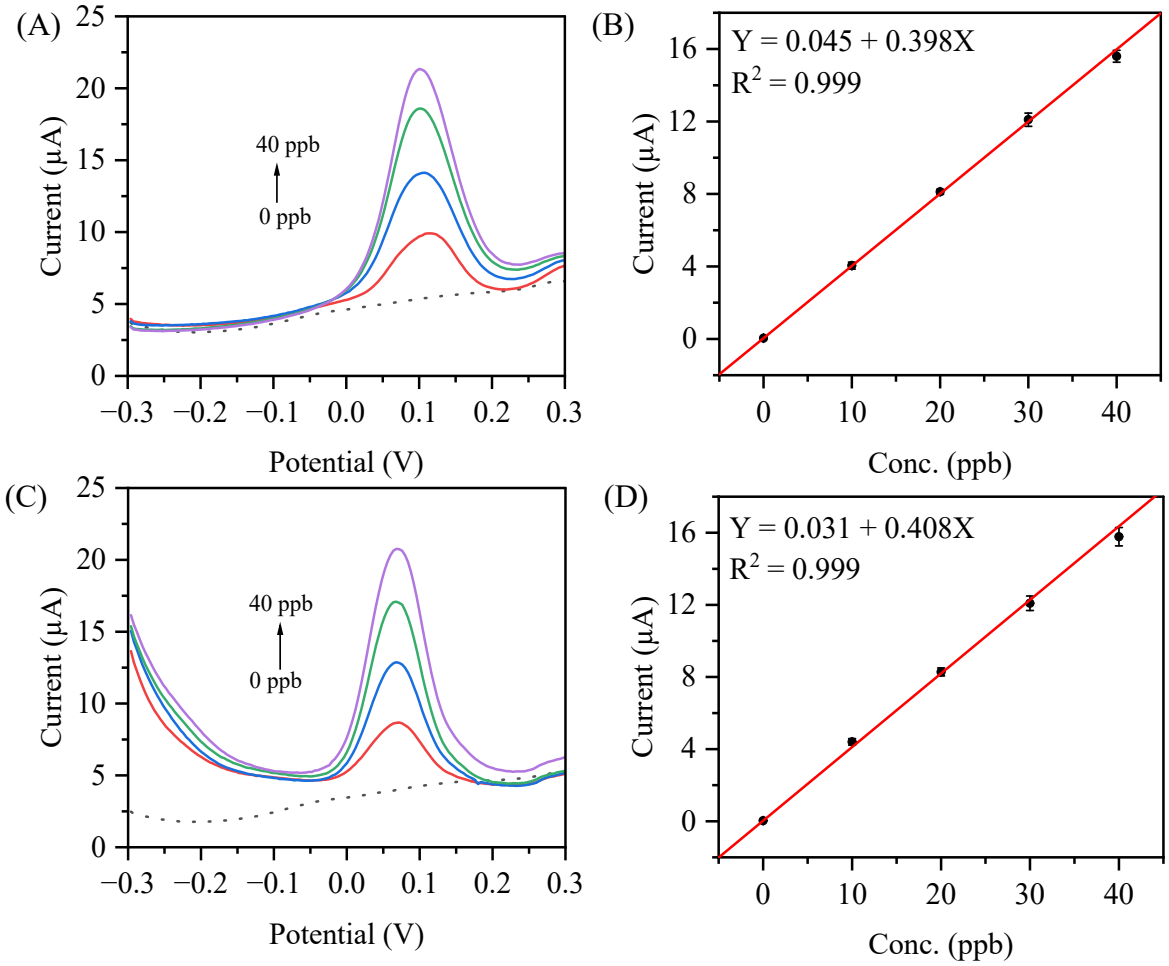

Fig. S11. SWASV responses of NG-AuCu/GCE for different concentrations of arsenic. (A) tap water, (C) mineral water, and (B and D) Corresponding calibration plot of peak current for arsenic concentrations (dotted line showing 0 ppb).

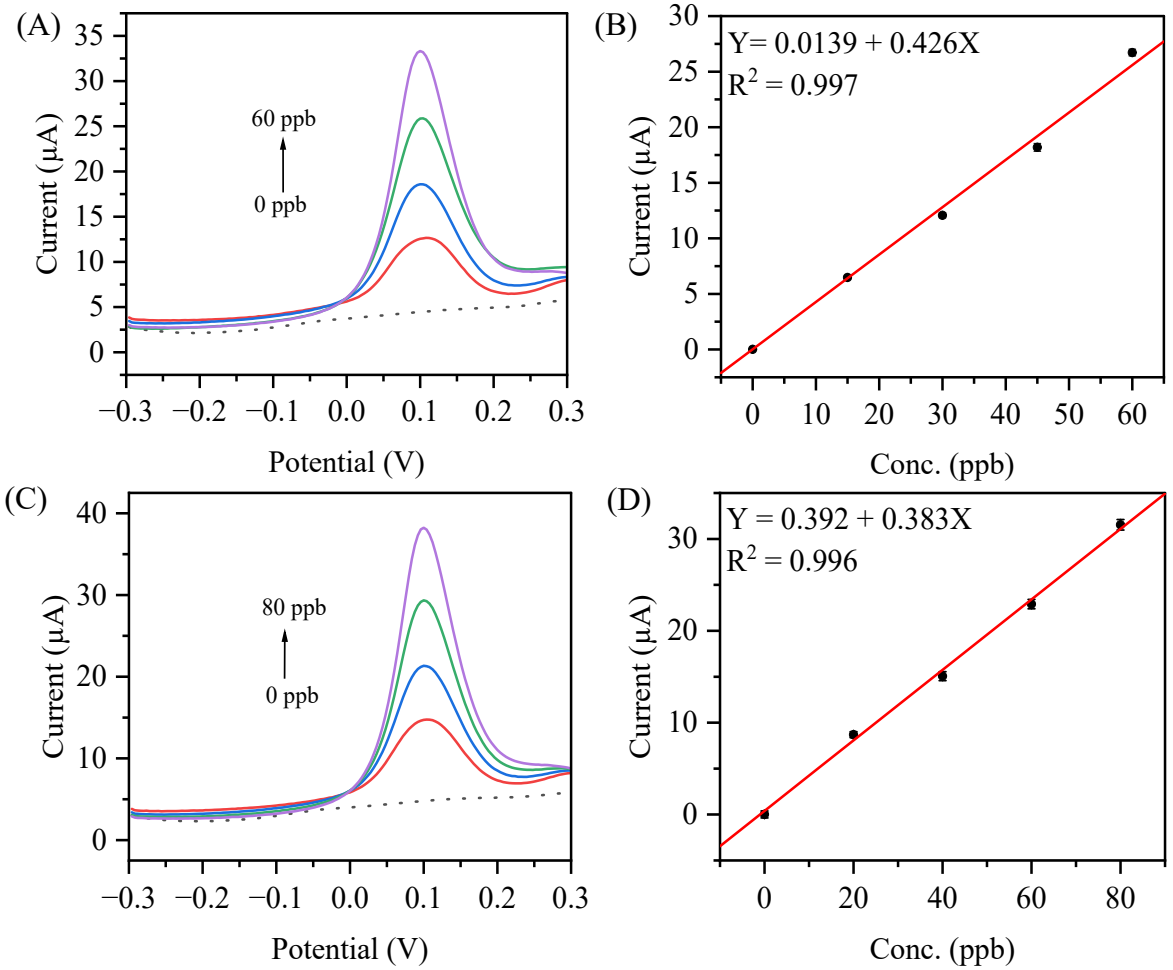

Fig. S12. SWASV responses of NG-AuCu/GCE for different concentrations of arsenic. (A) Fruit juice, (C) apple peel, and (B and D) Corresponding calibration plot of peak current for arsenic concentrations (dotted line showing 0 ppb).

References

1. Hu, J., et al., *Three-dimensional porous Au nanocoral structure decorated with Pt submonolayer via galvanic displacement of copper adatoms for electrooxidation of formic acid.* Russian Journal of Electrochemistry, 2016. **52**(4): p. 355-361.
2. Ren, B., et al., *The effect of electrodeposition parameters and morphology on the performance of Au nanostructures for the detection of As (III).* Journal of The Electrochemical Society, 2017. **164**(14): p. H1121.
3. Yang, L., et al., *Nano-Coral Gold (NCG) Electrode for Electrochemical Determination of Arsenic (III) in Industrial Wastewater by Square Wave Anodic Stripping Voltammetry (SWASV).* Analytical Letters, 2022. **55**(16): p. 2639-2649.
4. Yang, M., et al., *Reliable electrochemical sensing arsenic(III) in nearly groundwater pH based on efficient adsorption and excellent electrocatalytic ability of AuNPs/CeO2-ZrO2 nanocomposite.* Sensors and Actuators B: Chemical, 2018. **255**: p. 226-234.
5. Feeney, R. and S.P. Kounaves, *On-Site Analysis of Arsenic in Groundwater Using a Microfabricated Gold Ultramicroelectrode Array.* Analytical Chemistry, 2000. **72**(10): p. 2222-2228.
6. Gu, T., et al., *Dual-signal anodic stripping voltammetric determination of trace arsenic(III) at a glassy carbon electrode modified with internal-electrolysis deposited gold nanoparticles.* Electrochemistry Communications, 2013. **33**: p. 43-46.
7. Yang, M., et al., *Electrochemical determination of arsenic (III) with ultra-high anti-interference performance using Au–Cu bimetallic nanoparticles.* Sensors and Actuators B: Chemical, 2016. **231**: p. 70-78.